



Studies on retention of tritium implanted into tungsten by β -ray-induced X-ray spectrometry

M. Matsuyama ^{a,*}, T. Murai ^a, K. Yoshida ^a, K. Watanabe ^a,
H. Iwakiri ^b, N. Yoshida ^b

^a *Hydrogen Isotope Research Center, Toyama University, Gofuku 3190, Toyama 930-8555, Japan*

^b *Research Institute for Applied Mechanics, Kyushu University, Kasuga, Fukuoka 816-8580, Japan*

Abstract

Trapping and diffusion of tritium implanted into tungsten at room temperature were examined by β -ray-induced X-ray spectrometry. One of two thin tungsten plates used was previously irradiated with He ions. After the tritium irradiation, X-ray spectra from a W sample were measured in an argon atmosphere, and changes in the X-ray spectra with time were followed for five months at room temperature. The observed X-ray spectra consisted of three characteristic X-ray peaks and a bremsstrahlung X-ray peak. For the W sample without He pre-irradiation all characteristic X-ray intensities decreased with time, while those for the sample with He pre-irradiation were almost constant, indicating that the He irradiation strongly affects the migration of tritium. Furthermore, the X-ray spectra were analyzed by computer simulation to estimate a tritium depth profile. From those results, the diffusion coefficient of tritium at room temperature and effects of He pre-irradiation on trapping of tritium were evaluated.

© 2002 Elsevier Science B.V. All rights reserved.

1. Introduction

High-Z materials, especially tungsten and its alloys, are promising candidates for plasma facing components in the International Thermonuclear Experimental Reactor (ITER) as well as other future magnetic fusion devices. These materials have advantages of very high melting temperature, low vapor pressure, and very low sputtering erosion yield. The behavior of deuterium implanted into metals and high-Z materials has been reviewed by Myers et al. [1] and Yoshida [2]. However, there is still a lack of database of solubility, diffusivity and trapping of hydrogen isotopes in tungsten. Then it is of great importance to investigate in detail the retention and migration of tritium implanted into

high-Z materials from the viewpoints of fuel control and safety.

The present study focused the attention to effects of helium irradiation on the retention of tritium embedded in tungsten. The effects were examined by using a recently developed nondestructive measuring method, i.e., β -ray-induced X-ray spectrometry (BIXS). The new method has been applied so far to measure tritium on/in graphite [3], Pd and Zr [4,5], and the validity of this method has been confirmed. The main advantage of BIXS is that BIXS spectra can be observed without destroying samples. A BIXS spectrum is usually composed of two or more peaks of characteristic and bremsstrahlung X-rays. The intensity and shape of X-ray peaks depend not only on the amount of tritium captured on the surface and in subsurface layers but also on the depth profile of tritium in the bulk. Therefore, the amount and the depth profile can be determined with the aid of computer simulation.

This paper describes the dynamic behavior of trapping and migration of tritium ions implanted in tungsten

* Corresponding author. Tel.: +81-76 445 6926; fax: +81-76 445 6931.

E-mail address: masao@hrc.toyama-u.ac.jp (M. Matsuyama).

with the energy of 1 keV by BIXS measurements. Two different tungsten samples, with and without He pre-irradiation, were examined to compare the dynamic behavior of implanted tritium at room temperature.

2. Experimental

2.1. Materials

Two tungsten samples of $10 \times 10 \times 0.02 \text{ mm}^3$ prepared from thin polycrystalline tungsten plates (99.95% in purity) fabricated by powder metallurgy. One of the samples was applied to tritium irradiation at room temperature without any further treatments except for chemical cleaning (denoted as W(as-received)), and the other was irradiated with He ions at room temperature prior to tritium irradiation (denoted as W(He)). The diameter of the tritium irradiation spot was 6 mm. Energy and fluence of He ions were 8 keV and $5 \times 10^{21} \text{ ions m}^{-2}$, respectively. The He irradiation spot was an ellipse of $5 \times 3.5 \text{ mm}^2$.

An isotropic graphite plate was also used to monitor the tritium irradiation dose in each irradiation. The type and size of the graphite plate was IG-430U (Toyo Tanso Co.) and $15 \times 15 \times 0.5 \text{ mm}^3$, respectively. Tritium used in the present study was diluted with deuterium, and the tritium concentration was about 0.8%. The purities of deuterium and argon were 99.6% and 99.999%, respectively.

2.2. Tritium irradiation device

Tungsten samples containing tritium were prepared by using a tritium irradiation device. A schematic drawing of the tritium irradiation device is shown in Fig. 1. The apparatus consisted of three parts: an ultra-high vacuum part, a gas storage-supply part, and an ion implantation part. The first one was constructed by conventional vacuum pumps, and the residual pressure was routinely below $7 \times 10^{-7} \text{ Pa}$. The second part consisted of two tritium containers, a deuterium container, an argon cylinder, and a measuring device of tritium concentration by β -ray-induced X-ray counting in each implantation. One of the two tritium containers was subjected to supply and storage of tritium, and the other was used for recovery of tritium during the irradiation. Each container was loaded with a given amount of $\text{Zr}_9\text{Ni}_{11}$ alloy powder. The third part consisted of a sample holder fixed by a linear motion feedthrough, an ion gun (IG), a cold cathode gauge for the residual pressure measurements, and a quadruple mass spectrometer for residual gas analysis. The sample holder was equipped with an inner heater, and the holder was separable from the IG by use of a gate valve. A sputter

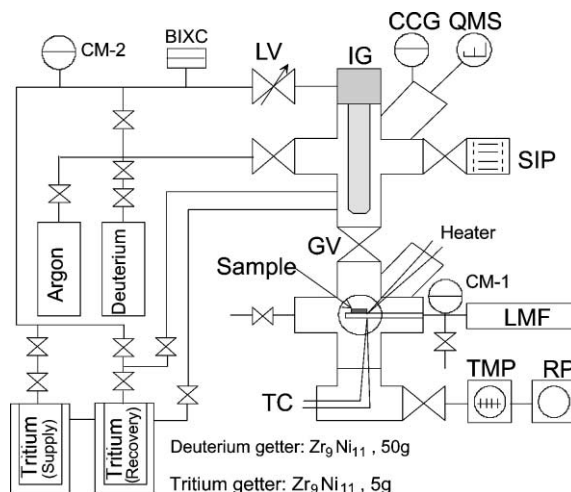


Fig. 1. Schematic of the tritium irradiation device.

ion pump (SIP) was used to minimize the release of residual tritium in the irradiation device.

2.3. X-ray measuring device

After tritium irradiation, the tritium-containing sample was moved to a separate X-ray measuring device equipped with an ultra-low energy X-ray detector. The detector was surrounded by two thick lead blocks (5 cm in thickness) to reduce the background level owing to natural radioactivity. During the measurement of an X-ray spectrum, the space between the sample and the detector (5 mm) was filled with a flow of argon to assay tritium retained on the surface and in surface layers as well as tritium implanted into the bulk. The details of an arrangement of the X-ray measuring device are described elsewhere [6].

2.4. Preparation of W samples containing tritium

The implantation of tritium ions in a W sample was carried out as follows. After the W sample was set at the sample holder equipped with the tritium irradiation device, it was heated in vacuum at 673 K for 1 h. The sample was irradiated with tritium ions for 15 min under a constant tritium pressure of 4 Pa. During irradiation, the ion current was measured by applying the bias of +18 V to the sample to reduce emission of secondary electrons. The observed ion current was kept constant at about $1 \mu\text{A}$. Prior to takeout of the irradiated sample from the tritium irradiation device, the irradiation device was evacuated by a SIP for about one week to minimize the release of tritium adsorbed on the inner wall surface. After the evacuation, the device was decontaminated by employing a conventional tritium decontamination device, and then the irradiated sample

was taken out and kept in an ambient atmosphere at room temperature (300 ± 2) K except for a period of measurements.

3. Results and discussion

3.1. An example of X-ray spectra observed

The maximum energy of β -rays of tritium atoms is 18.6 keV. It is enough to excite electrons in an atom. Fig. 2 shows an example of X-ray spectra observed for the W sample (as-received). Two kinds of X-ray peaks appeared: one are characteristic X-rays of Ar($K\alpha$), W($L\alpha$) and W($M\alpha$), and the other are bremsstrahlung X-rays which were generated by interactions between β -rays and tungsten atoms. The intensity of the Ar($K\alpha$) peak reflects the amount of tritium retained on the surface and in subsurface layers; subsurface means the range of the escape depth of β -rays in tungsten. The intensities of W($L\alpha$) and W($M\alpha$) strongly varies with the amount of tritium, but the ratio between them depends on the depth profile of tritium because of the difference in penetration power of each X-rays. On the other hand, the intensity of the broad bremsstrahlung X-ray peak is affected by the total amount of tritium in the bulk. In

addition, the peak shape mainly depends on a tritium depth profile because the attenuation fraction of X-rays in a material is strongly dependent on the distance from the surface to the generation point of X-rays as well as the energy of X-rays. Therefore, changes in intensity of characteristic X-rays and in shape of bremsstrahlung X-rays give information about the dynamic behavior of tritium in tungsten.

3.2. Changes in intensity of characteristic X-ray peaks for W(as-received) and W(He) samples

Information on tritium concentration in a certain depth is reflected to the intensities of each characteristic X-rays. For example, the X-rays of Ar($K\alpha$) are mainly induced by direct interactions with β -rays emitted from the surface and/or subsurface layers of tungsten. Namely, the intensity of Ar($K\alpha$) gives information about the concentration of tritium existing within the average escape depth (≈ 50 nm) of β -rays in tungsten. On the other hand, the penetration depth of W($L\alpha$) and W($M\alpha$) X-rays is far larger than that of β -rays. The intensities of those X-rays, therefore, provide information up to a deep region of an order of micrometer. The intensity of W($M\alpha$) X-rays depends on the amount of tritium up to a depth of about 1 μm , while that of W($L\alpha$) X-rays depends on a depth of about 10 μm . Attenuation profiles of characteristic X-rays and β -rays in tungsten are shown in Fig. 3. The attenuation coefficients of X-rays were cited from the literature [7], and that of β -rays was determined from other experiments.

Figs. 4 and 5 show changes in the intensity of each characteristic X-ray peak observed for W(as-received) and W(He) samples, respectively. Two fairly different features appeared in both samples: namely, one is the initial intensity of each X-rays, and the other is an intensity change with time. Although the tritium fluence in each irradiation was almost the same for both samples, the initial X-ray intensities for the W(as-received) sample were several times lower than those for the W(He) sample. This indicates that the amount of tritium increased by He pre-irradiation. This increase should be due to the change in trapping energy of tritium on/in tungsten, because a variety of defects such as dislocations, vacancies and helium bubbles can be produced by He pre-irradiation. The increase in the tritium inventory in tungsten is a severe problem for controlling fuel balance and tritium safety. Furthermore, the change in the intensity ratio of W($L\alpha$) to W($M\alpha$) with time was quite different. A gradual increase of the ratio appeared in the W(as-received) sample, whereas in the W(He) sample the ratio was almost constant within the experimental period. The increase in the ratio indicates that the tritium depth profile just after irradiation gradually changed with time by diffusion of tritium atoms into the bulk.

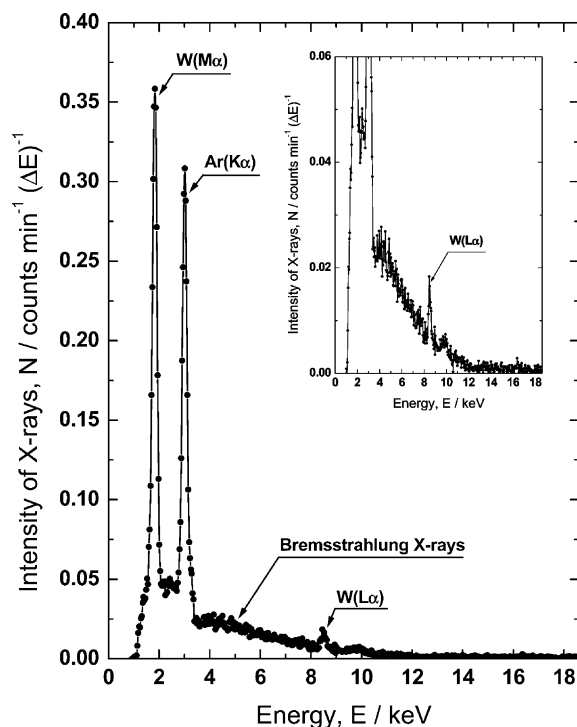


Fig. 2. Typical X-ray spectrum observed for tungsten sample containing tritium.

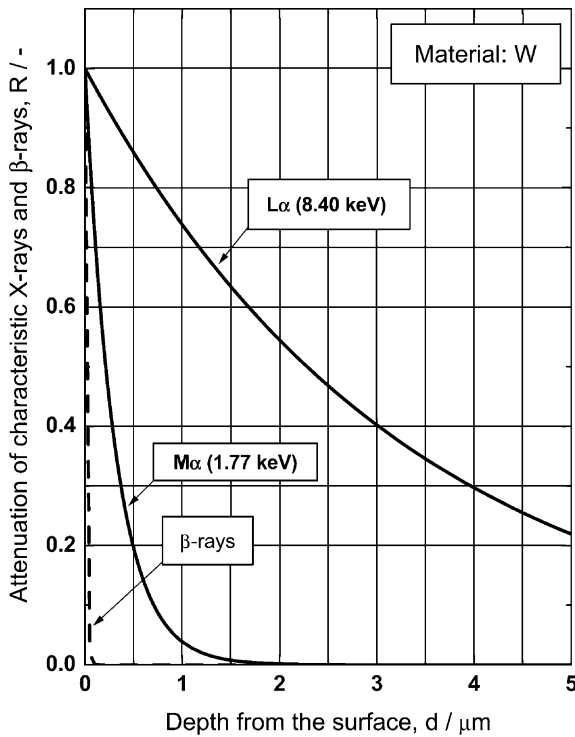


Fig. 3. Attenuation of β -rays and characteristic X-rays in tungsten sample.

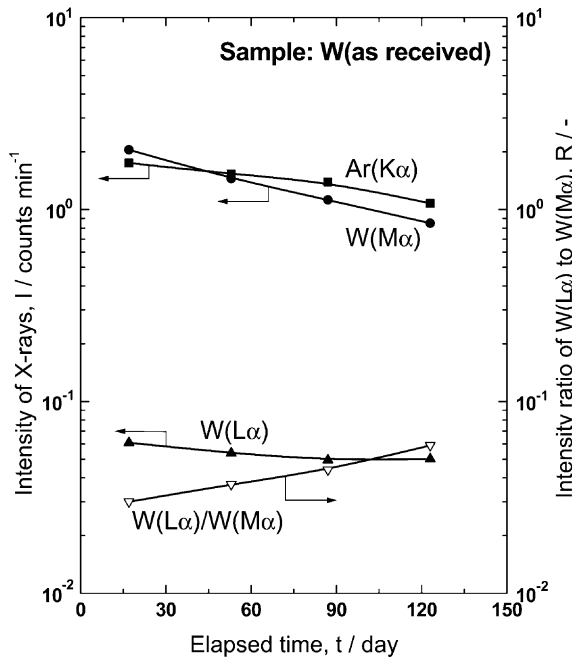


Fig. 4. Changes in X-ray intensities and intensity ratio $W(M\alpha)/W(L\alpha)$ for W(as-received) sample.

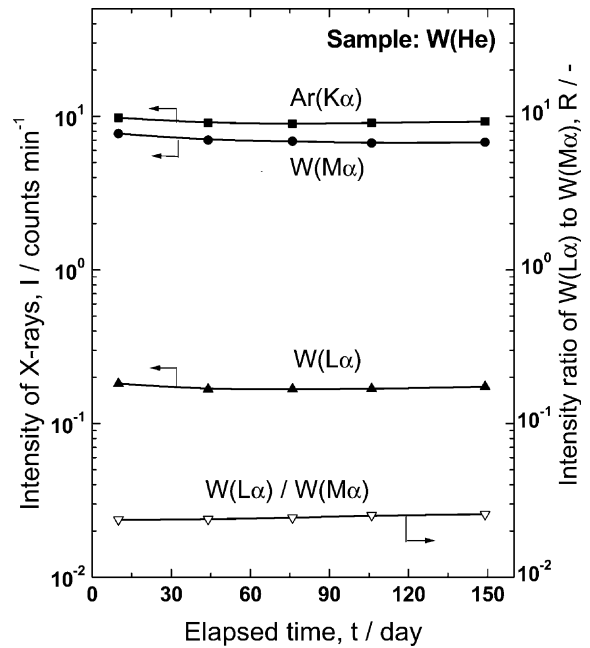


Fig. 5. Changes in X-ray intensities and intensity ratio $W(M\alpha)/W(L\alpha)$ for W(He) sample.

3.3. Analysis of X-ray spectra by computer simulation

It is possible to reproduce an observed X-ray spectrum by taking account of generation of characteristic and bremsstrahlung X-rays and attenuation of X-rays in a tritium containing material. The details of computer simulation are described elsewhere [8]. Fig. 6 shows a typical simulation spectrum along with the observed one for the W(as-received) sample. The observed spectrum was measured on the 17th day after tritium irradiation. The enlarged bremsstrahlung X-ray spectrum is shown in the inset of the figure. The parameter in the simulation process is only a depth profile of tritium. The simulation spectrum drawn by a solid line in Fig. 6 was calculated based on the tritium depth profiles as illustrated in Fig. 7. The simulation spectrum agreed very well with the observed spectrum, indicating that the irradiated tritium ions diffused into the bulk. To examine the effects of He pre-irradiation, the tritium depth profile for W(He) sample is also illustrated in Fig. 7. These profiles were obtained from the first measurements of X-ray spectra after tritium irradiation for both samples. As for W(He) the tritium depth profile is expected to be unchanged with time, because little change in the intensity and shape of X-ray spectra for the W(He) sample was observed during a run. Both profiles in Fig. 7 are quite different from each other, and for the W(He) sample it can be understood that most of the implanted tritium was strongly trapped near a surface region below

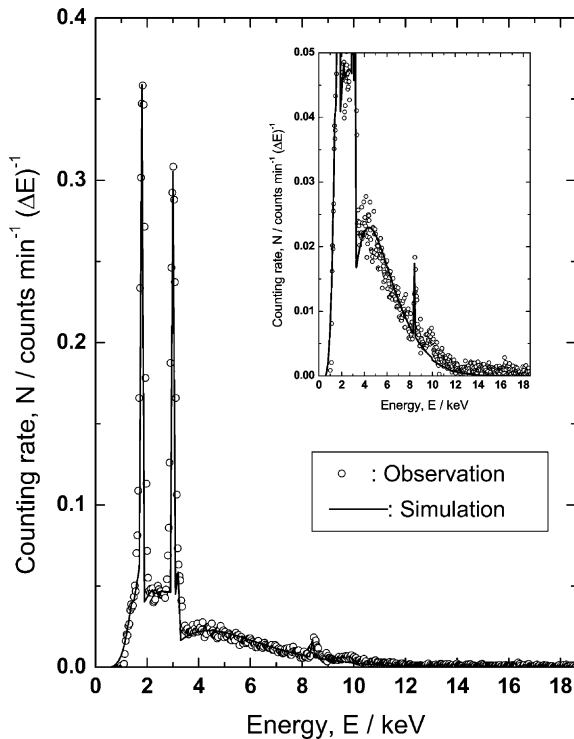


Fig. 6. Comparison of the simulated spectrum with the observed spectrum on the 17th day after tritium irradiation for W(as-received) sample.

100 nm. This coincides with the formation of He bubbles near the surface region under the present He pre-irradiation conditions.

3.4. Estimation of the diffusion coefficient of tritium in W(as-received) sample

To estimate the diffusion coefficient of tritium at room temperature in a W(as-received) sample, the simulation analysis was carried out for X-ray spectra observed, and then a tritium depth profile at each time was determined as four lines in Fig. 8. It was seen that the initial tritium distribution extended to bulk with time. From the change in these depth profiles, to evaluate the diffusion coefficient of tritium, tritium depth profiles expected from a given diffusion coefficient were calculated, which were shown by the closed circles on each line. In this calculation, it was assumed that a sample is a semi-infinite medium, and desorption of tritium from the surface is negligibly small. The depth profiles determined from the observed X-ray spectra could be reproduced very well by the diffusion calculation adopting a considerably small diffusion coefficient, $2.4 \times 10^{-19} \text{ m}^2 \text{ s}^{-1}$. This value is an effective diffusion coefficient because the present tungsten sample inherently contains

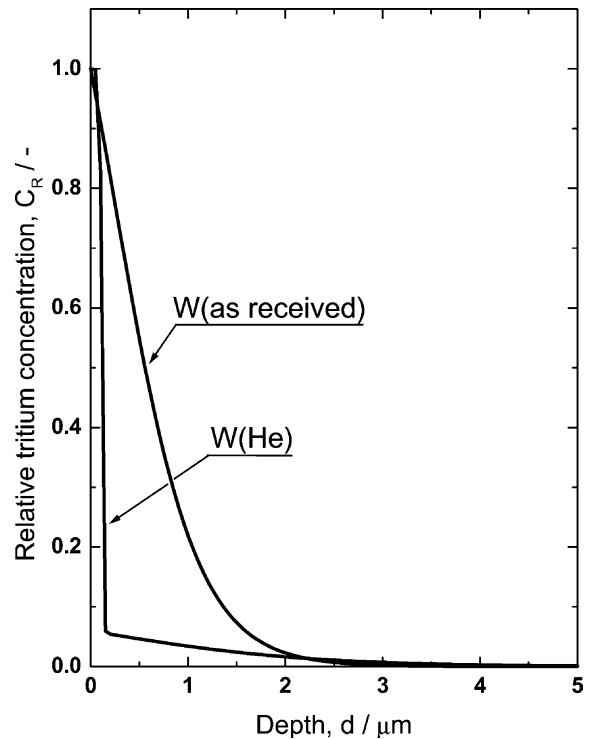


Fig. 7. Initial tritium depth profiles estimated by computer simulation for both samples.

natural traps for hydrogen isotopes [9]. For a W(He) sample, on account of little change in the X-ray spectra observed, it was hard to evaluate the change in a tritium depth profile.

Although the diffusion constant of hydrogen in tungsten has been measured so far at higher temperatures above 1000 K [10–12], there are no data determined at low temperatures. Namely, the present value determined by BIXS is the first result at room temperature. The temperature dependence of the diffusion coefficient and the trapping energy of tritium in the W(He) sample will be reported in the near future.

4. Summary

The dynamic behavior of tritium implanted into two kinds of tungsten samples, W(as-received) and W(He), was examined by the newly developed BIXS. The amount of tritium retained on/in the materials and the depth profile of tritium could be evaluated by using BIXS. The changes of the intensity and the shape of an X-ray spectrum observed in a tungsten sample were followed for about five months at room temperature. The results are summarized as follows:

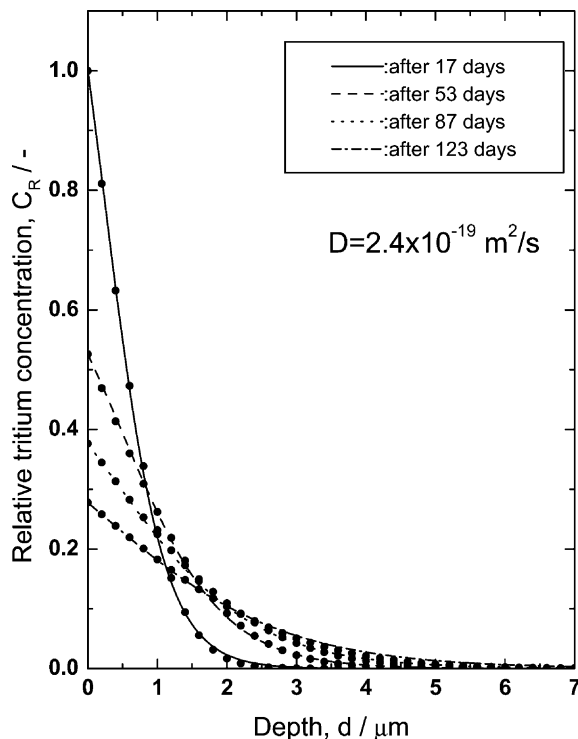


Fig. 8. Comparison between depth profiles determined by BIXS analyses and diffusion calculation.

- (1) Two kinds of X-rays appeared in each spectrum: namely, one are the characteristic X-ray peaks such as $\text{Ar}(K\alpha)$, $\text{W}(L\alpha)$ and $\text{W}(M\alpha)$, and the other is a broad bremsstrahlung X-ray peak.
- (2) The intensities of the characteristic X-rays in the W(as-received) sample decreased with time, and in addition the ratio $\text{W}(M\alpha)/\text{W}(L\alpha)$ increased gradually, indicating that most of the implanted tritium moved in the bulk with time.
- (3) On the contrary, for the W(He) sample the intensities of $\text{W}(L\alpha)$ and $\text{W}(M\alpha)$ X-rays and the ratio between them changed very little during the measurement. Furthermore, the initial intensities of characteristic X-ray peaks of the W(He) sample were

several times higher than those for the W(as-received) sample. These indicate that the implanted tritium is strongly trapped in the implantation zone of helium.

- (4) The numerical analysis of an X-ray spectrum with the aid of computer simulation was carried out basing on a given depth profile of tritium in the W(as-received) sample. From the depth profiles estimated by computer simulation, the effective diffusion coefficient of tritium was evaluated to be $2.4 \times 10^{-19} \text{ m}^2 \text{ s}^{-1}$ at room temperature.

Acknowledgement

This work was partly supported by the grant-in-aid for Scientific Research from the Ministry of Education, Culture, Sports, Science and Technology of Japan.

References

- [1] S.M. Myers, P.M. Richards, W.R. Wampler, F. Besenbacher, *J. Nucl. Mater.* 165 (1989) 9.
- [2] N. Yoshida, *J. Nucl. Mater.* 266–269 (1999) 197.
- [3] M. Matsuyama, T. Tanabe, N. Noda, V. Philipps, K.H. Finken, K. Watanabe, *J. Nucl. Mater.* 290–293 (2001) 437.
- [4] M. Matsuyama, S. Ueda, K. Watanabe, *Ann. Rept. Hydrogen Isotope Res. Center, Toyama Univ.* 19 (1999) 33.
- [5] M. Matsuyama, S. Ueda, K. Watanabe, *Fusion Eng. Des.* 49&50 (2000) 885.
- [6] M. Matsuyama, S. Ueda, T. Ogawa, T. Uda, K. Watanabe, *Ann. Rept. Hydrogen Isotope Res. Center, Toyama Univ.* 18 (1998) 69.
- [7] D.R. Lide, in: *CRC Handbook of Chemistry and Physics*, 76th ed., CRC, Tokyo, 1995, p. 10.
- [8] M. Matsuyama, K. Watanabe, K. Hasegawa, *Fusion Eng. Des.* 39–40 (1998) 929.
- [9] P. Franzen, C.G. Rosales, H. Plank, V.Kh. Alimov, *J. Nucl. Mater.* 241–243 (1997) 1082.
- [10] L.N. Ryabchikov, *Ukr. Fiz. Zh.* 9 (1964) 293.
- [11] G.E. Moore, F.C. Unterwald, *J. Chem. Phys.* 40 (1964) 2639.
- [12] R. Frauenfelder, *J. Vac. Sci. Technol.* 6 (1969) 388.